Pergamon

Int. J. Solids Structures Vol. 31, No. 7, pp. 971–984, 1994

0020–7683/94 $6.00 + .00

A NUMERICAL ANALYSIS OF CYCLIC CREEP FRACTURE

M. L. AYARI and B. K. SUN
Department of Mechanical and Industrial Engineering, University of Manitoba, Winnipeg, Manitoba, Canada R3T 2N2

and

T. R. HSU
Department of Mechanical Engineering, San Jose State University, San Jose, CA 95192-0087, U.S.A.

(*Received* 11 *February* 1993; *in revised form* 14 *June* 1993)

Abstract—A new continuum damage mechanics (CDM) based model for describing cyclic creep behavior of selected engineering materials under complex thermal-mechanical loading conditions is incorporated into a finite element computer code for cyclic creep fracture analysis. A mixed explicit-implicit (EI) algorithm was used to deal with the evolution of creep damage in the material. Three case studies were conducted on a cracked thin panel made of 316L stainless steel. Loading conditions for these case studies correspond to static, cyclic without dwell time and cyclic with dwell time, respectively. Mechanical load and temperature changes applied in phase with each other are considered in this investigation. Numerical results indicate that both the load dwell time and the loading/unloading cycling process have profound influence on subsequent creep behavior.

NOMENCLATURE

K	stress intensity factor
ΔK	stress intensity factor range
J	J integral
C^*	C^* parameter
Q^*	Q^* parameter
CTOD	Crack Tip Opening Displacement
σ_{net}	net section stress
σ_{ij}	stress tensor component
T	absolute temperature
D	damage parameter
$\mathbf{R}_{ij}$	internal stress tensor
R	Boltzmann constant
ε^c, ε^c_{ij}	creep strain, creep strain tensor
$(\dot{\cdot})$	time derivative operator
t	time
S_{ij}	deviatoric stress component
$\tilde{\sigma}$	damage equivalent stress
$\bar{R}$	effective internal stress in von Mises sense
$\bar{\sigma}$	effective stress in von Mises sense
R_s	current maximum internal stress
R^o_s	initial maximum internal stress
R^u, R^u_{ij}	internal stress during unloading
R^r, R^r_{ij}	residual internal stress before unloading
$\dot{D}_c$	creep damage rate
ΔD_f	fatigue damage increment
Δt_d	length of dwell time
σ_H	hydrostatic stress
$\Delta\varepsilon_p$	plastic strain range in load cycling process
E	Young's modulus
ν	Poisson's ratio
Q	activation energy
N	number of load cycles
σ_n	creep threshold stress value
$\partial f/\partial N$	fatigue damage rate
$A, n, m, B_1, p, C_1, C_2, r_0, \alpha, \beta, B_2, k, c_0, B$	material constants dependent upon temperature
A_1, A_2, B_3, B_4	material constants
γ	constant in numerical one step integration formulae
CDM	Continuum Damage Mechanics
EI	Explicit-Implicit
LCF	Low Cycle Fatigue
HTLCF	High Temperature Low Cycle Fatigue.

INTRODUCTION

In pursuit of thermal efficiency, key components in electric power generation, aerospace, and petrochemical plants are exposed to high temperature environment with high stresses. Under the working conditions, these components experience significant creep deformation. Creep damage is one of the prominent mechanisms leading to the failure of these components.

Large scale investigations in creep mechanics in general and creep fracture mechanics in particular had been conducted in the past three decades, and much progress had been achieved [Boyle and Spence (1983), Rabotnov (1969), Odqvist (1980), Leckie (1980) and Hsu (1986)]. Generally speaking, besides the conventional mechanics way of describing creep behavior, two schools of thought in treating creep-related problems have emerged: the parametric approach and the CDM approach.

The parametric approach is an extension of the conventional fracture mechanics framework to creep analysis [Nicholson and Formby (1975), Landes and Begley (1976), Smith *et al.* (1989), Leeuwen (1977) and McEvily and Wells (1973)]. The characterizing feature of the parametric methods pertains to the use of one single control parameter which the formulation of decision is based on, such as the stress intensity factor, K, the stress intensity factor range, ΔK, the J integral, the C^* parameter [Sexena (1980) and Nikbin *et al.* (1976)], the Q^* parameter [Yokobori and Sakata (1979) and Yokobori and Yokobori (1988)], the crack tip opening displacement, CTOD, and the nominal stress or the net section stress, σ_{net}, etc. Parametric approaches achieved certain degrees of success in correlating creep data with one of the parameters for particular materials under certain conditions. However, most of the parameters are valid only for the steady-state creep deformation. This is obviously inadequate because creep rupture depends on all stages of creep deformation, including the primary and tertiary stages. For cases involving complex temperature and stress histories, the creep problem becomes very complicated. Additional complexities are the load cycling effect, the load dwell time effect and the interaction between creep and high temperature low cycle fatigue (HTLCF). One single parameter cannot possibly take all these effects into account. The applicability of parametric approach for creep-fracture analysis is thus limited.

The CDM approach involves internal state variables such as the damage parameter and the internal stress in describing the current state of the material and its capacity to undertake the applied load. These variables are introduced on the basis of conventional mechanics. The damage parameter is an abstract indication of material deterioration due to permanent deformation. Many different researchers, such as Gong and Hsu (1991), Leckie and Hayhurst (1974), Kachanov (1958), Rabotnov (1969), Krajcinovic and Fonseka (1981), Chaboche (1988), Lemaitre (1985), Miller (1976), Chow and Wang (1987), Murakami (1983), etc., proposed different CDM models to describe material behavior under different conditions. Some of these proposed models are too complicated in form to be of practical use. Others require a large number of material constants which are usually difficult to obtain in practice. Also, only a few of the models take into account critical factors such as the dwell time effect, the interaction between creep and HTLCF and the load cycling effect in the cyclic creep fracture analysis.

Recently, the authors proposed a CDM based model for describing creep behavior of selected engineering materials subjected to complex stress and temperature histories. This model can also describe load cycling effect, load dwell time effect and the interaction between creep and HTLCF [Sun *et al.* (1992)]. This present paper is concerned with the implementation of this model into an existing finite element program, TEPSAC [Hsu (1986)], and the stress analysis results of three case studies on cracked thin panel made of 316L stainless steel.

Computations involving CDM models for creep analysis are usually difficult due to the high nonlinearity and mathematical stiffness of the governing equations. The mathematical stiffness comes from the fact that the CDM models for creep analysis are usually written in a rate form. The creep strain rate and the damage rate are all functions of the current stress, σ, temperature, T, and state variables such as the damage parameter, D, and the internal stress, R. Hence, slight perturbations in σ, T and the state variables can cause relatively large variations in both the creep strain rate and the damage rate. This imposes very small time increments in order to maintain accurate and stable progress of the solutions.

It is thus not surprising that many researchers were involved in the study of algorithms for tackling the mathematical stiffness of nonlinear problems. Some improved algorithms have been proposed [Chen and Hsu (1988), Hughes and Liu (1978), Cormeau (1975) and Liu *et al.* (1982)]. Chen and Hsu proposed a mixed explicit-implicit (EI) algorithm for creep stress analysis. This algorithm can achieve both economical computation and yet ensure numerical stability. In this paper, the proposed model is incorporated into a finite element program using this mixed EI algorithm.

The breakable element algorithm [Hsu (1986)] is adopted in this paper to simulate crack growth. The Mroz hardening rule in conjunction with the multiple yield surface theory [Mroz (1967)] is utilized to account for the progress of yielding in the analysis.

THEORETICAL BACKGROUND

Constitutive equations

A new CDM based model was proposed to describe creep behavior of selected engineering materials under cyclic thermal-mechanical loading conditions (with both load holding time and load dwell time). The model is the synthesis of the works of Gong and Hsu (1991), Degallaix *et al.* (1983), Lemaitre (1985), Chaboche (1988) and Plumtree (1977). The mathematical form of the model is presented below:

$$\dot{\varepsilon}_{ij}^{c} = A\left(\frac{\tilde{\sigma}-\bar{R}}{1-c_o D}\right)^{n}\frac{S_{ij}}{\tilde{\sigma}}, \tag{1}$$

$$\dot{\mathbf{R}}_{ij} = B_1(R_s-\bar{R})^{p}\dot{\varepsilon}_{ij}^{c}, \tag{2}$$

$$\dot{D}_c = C_1\frac{\tilde{\sigma}}{1-D}+C_2\left(\frac{\tilde{\sigma}-\bar{R}}{1-D}\right)^{r_o n}\left(\frac{\tilde{\sigma}}{1-D}\right)^{r_o}, \tag{3}$$

and:

$$R_s = R_s^o\left[1+\beta\left(\frac{\tilde{\sigma}-\bar{R}}{\tilde{\sigma}}\right)\Delta t_d\right]^{\alpha} \tag{4}$$

for unloading:

$$\dot{R}_{ij}^{u} = B_2(R_{ij}^{r}-R_{ij}^{u})^{k}, \tag{5}$$

and:

$$\tilde{\sigma} = \bar{\sigma}\left[\frac{2}{3}(1+\nu)+3(1-2\nu)\left(\frac{\sigma_H}{\bar{\sigma}}\right)^{2}\right]^{1/2}, \tag{6}$$

$$\Delta D_f = A_1(\Delta\varepsilon_p)^{B_3}\mathrm{e}^{-Q/RT}+A_2(\Delta\varepsilon_p)^{B_4}, \tag{7}$$

$$\Delta D = \dot{D}_c\,\mathrm{d}t+\frac{\partial D_f}{\partial N}\mathrm{d}N. \tag{8}$$

In this model, the first six equations, eqns (1–6) are used to describe the creep behavior of selected engineering materials, including the accumulation of damage and the internal stress histories. These equations are mainly an extension of Gong and Hsu's uniaxial model to the three dimensional case. Equation (6) defines a generalization of the damage equivalent stress. According to Lemaitre, who first introduced this concept, the damage equivalent stress in CDM analysis is the counterpart of the von Mises effective stress in plasticity analysis. Equation (7) is used to calculate the damage caused in the load cycling process. This is an adaptation of the Degallaix's thermal activation model. In this way, the damage caused by the LCF process is calculated cycle by cycle. Instantaneous response such as strain hardening and softening is accounted for. The damage produced by LCF and creep deformation are introduced in a mutually reinforcing manner as expressed by eqn (8).

Time-integration scheme

Generally speaking, there are two classes of commonly used one-step integration algorithms for creep computation: explicit and implicit algorithms. Implicit algorithms tend to be numerically stable, permitting larger time steps, however, the computational cost per time step is substantial. Explicit algorithms are simple in form and involve inexpensive marching strategies, but numerical stability requires that a very small time step be employed. The selection of the time-integration algorithm depends on whether the short term or long term response is of interest. There are some problems for which implicit algorithms are very efficient and others for which explicit algorithms are very efficient. However, in large scale engineering systems, the many different finite element types and local mesh refinement often result in neither class of integration algorithms being very efficient by itself.

To circumvent these difficulties, methods have been developed in which it is attempted to simultaneously take advantage of the benefits of both types of algorithms. The mixed explicit-implicit (EI) algorithm originally proposed by Hughes *et al.* (1978) and Liu *et al.* (1982) for structural dynamics and nonlinearity has been applied to creep stress analysis [Chen and Hsu (1988)]. This has led to significant computational advantage.

When the mixed EI algorithm is used in a finite element analysis, the mesh is partitioned into an implicit element group and an explicit element group. Within each group, a separate integration algorithm is adopted. Different time stepping can be used at the same time for each element group. In the implicit group, a limited Taylor series expansion technique is introduced to evaluate the rates of creep deformation and certain internal variables at the end of the time step.

Finite element equations

In finite element analysis of the thermal-elastic–plastic response with creep, the following decomposition is usually made:

$$\{\Delta\varepsilon\} = \{\Delta\varepsilon_e\} + \{\Delta\varepsilon_p\} + \{\Delta\varepsilon_T\} + \{\Delta\varepsilon_c\}, \tag{9}$$

where $\{\Delta\varepsilon\}$, $\{\Delta\varepsilon_e\}$, $\{\Delta\varepsilon_p\}$, $\{\Delta\varepsilon_T\}$ and $\{\Delta\varepsilon_c\}$ are respective total, elastic, plastic, thermal and creep strain increments. Incremental quantities are used here to linearize the apparent nonlinear material behavior under combined thermal-mechanical loadings during a time step Δt of a load increment. The separation of plastic and creep strain increments is obviously an artificial one, since they are both related to the dislocation movements within the material. Many researchers, however, have shown that this assumption is a convenient and reasonable one [Levy and Pifko (1981)] since a plastic strain increment is associated with high rates of loading. Hence, the plastic strain component is configured to be time independent, and is regarded as instantaneous response when the loading process is quick enough in comparison with the creep process.

In this contribution, the thermal strain and creep strain are treated separately. Since the temperature change is in-phase with the application of the mechanical load, i.e. changes rapidly relative to the long holding time and the dwell time of the loads, it is reasonable to treat the thermal effects as instantaneous and to assume that no creep can occur during the thermal-mechanical loading/unloading span of time. The well-established thermal elastic–plastic theory [Hsu (1986)] is used for the analysis of the instantaneous response.

When creep deformation is included in the thermal elastic–plastic finite element analysis, the stress increment during a time step Δt is given by:

$$\{\Delta\sigma\} = [C_{ep}](\{\Delta\varepsilon\} - \{\Delta\varepsilon_c\}) \tag{10}$$

where $[C_{ep}]$ is the thermal elastic–plastic matrix.

By introducing the strain–displacement relation:

$$\{\Delta\varepsilon\} = [B]\{\Delta u\} \tag{11}$$

the stress increment is calculated using:

$$\{\Delta\sigma\} = [C_{ep}]([B]\{\Delta u\} - \{\Delta\varepsilon_c\}) \tag{12}$$

and the incremental equilibrium during a time step is given by:

$$\int_v [B]^T\{\Delta\sigma\}\,\mathrm{d}v = \{\Delta F\}. \tag{13}$$

In practice, the evaluation of $\{\Delta\sigma\}$ is first performed and the subsequent finite element solutions depend on whether the element in question belongs to the explicit or implicit group.

Finite element modelling of CDM

In the implementation of the mixed (EI) algorithm, the finite element mesh is partitioned into two groups: the explicit element group and the implicit element group. Integration in each of the two element groups is performed independently.

Explicit element group. The increments of creep strain $\{\Delta\varepsilon_c\}$, damage parameter ΔD and internal stress $\{\Delta R\}$ occurring in a time interval $\Delta t = t_{n+1} - t_n$ are evaluated as:

$$\{\Delta\varepsilon_c\} = \{\dot{\varepsilon}_c^n\}\Delta t, \tag{14}$$

$$\Delta D = \dot{D}^n\Delta t, \tag{15}$$

$$\{\Delta R\} = \{\dot{R}^n\}\Delta t, \tag{16}$$

where the superscript n denotes the time step number. The stress increment can then be expressed by substituting eqn (14) into eqn (12) as follows:

$$\{\Delta\sigma\} = [C_{ep}]([B]\{\Delta u\} - \{\dot{\varepsilon}_c^n\}\Delta t). \tag{17}$$

The governing finite element equation now becomes:

$$\left(\int_v [B]^T[C_{ep}][B]\,\mathrm{d}v\right)\{\Delta u\} = \int_v [B]^T[C_{ep}]\{\dot{\varepsilon}_c^n\}\Delta t\,\mathrm{d}v + \{\Delta F\}, \tag{18}$$

where $\{\Delta F\}$ is given in eqn (13). Hence, in order to trace the creep response, simple update of the right hand side is performed and the solution is achieved by marching in time. The matrix $\int_v [B]^T[C_{ep}][B]\,\mathrm{d}v$ is evaluated only at the first time step.

Implicit element group. According to the proposed model, eqns (1–8), we have:

$$\{\dot{\varepsilon}^c\} = f_1(\{\sigma\}, \{R\}, D) \tag{19}$$

$$\{\dot{R}\} = f_2(\{\sigma\}, \{R\}, D) \tag{20}$$

$$\dot{D} = f_3(\{\sigma\}, \{R\}, D). \tag{21}$$

One-step integration formulae used to calculate the increments of creep strain, damage parameter and the internal stress from this set of rates are then given by the following finite difference equations:

$$\{\Delta\varepsilon_c\} = [(1-\gamma)\{\dot{\varepsilon}^c_n\} + \gamma\{\dot{\varepsilon}^c_{n+1}\}]\Delta t, \tag{22}$$

$$\Delta D = [(1-\gamma)\dot{D}_n + \gamma\dot{D}_{n+1}]\Delta t, \tag{23}$$

$$\{\Delta R\} = [(1-\gamma)\{\dot{R}_n\} + \gamma\{\dot{R}_{n+1}\}]\Delta t. \tag{24}$$

The creep strain rate $\{\dot{\varepsilon}^c_{n+1}\}$ and the two state variables: $\dot{D}_{n+1}$ and $\{\dot{R}_{n+1}\}$ at the time point t_{n+1} can be approximated by a limited Taylor series expansion as:

$$\{\dot{\varepsilon}^c_{n+1}\} \approx \{\dot{\varepsilon}^c_n\} + [\mathbf{H}_1]\{\Delta\sigma\} + [\mathbf{H}_2]\{\Delta R\} + \{\mathbf{H}_3\}\Delta D, \tag{25}$$

$$\dot{D}_{n+1} \approx \dot{D}_n + \{\mathbf{G}_1\}\{\Delta\sigma\} + \{\mathbf{G}_2\}\{\Delta R\} + \mathbf{G}_3\Delta D, \tag{26}$$

$$\{\dot{R}_{n+1}\} \approx \{\dot{R}_n\} + [\mathbf{E}_1]\{\Delta\sigma\} + [\mathbf{E}_2]\{\Delta R\} + \{\mathbf{E}_3\}\Delta D, \tag{27}$$

where $[\mathbf{H}_1]$, $[\mathbf{H}_2]$, $\{\mathbf{H}_3\}$, $[\mathbf{E}_1]$, $[\mathbf{E}_2]$, $\{\mathbf{E}_3\}$, $\{\mathbf{G}_1\}$, $\{\mathbf{G}_2\}$, $\mathbf{G}_3$ are transformation matrices, vectors and coefficients used in the derivation.

Thus, by substituting eqns (23–27) into eqn (22), we obtain the incremental creep strain components. Substituting the outcome into eqn (10), we obtain the incremental stress components. Again, using eqn (10) and expressing incremental equilibrium leads to the governing finite element equation with the new model incorporated, which has the following form:

$$\left(\int_v [B]^T[C^*_{ep}][B]\,\mathrm{d}v\right)\{\Delta u\} = \{\Delta F\} + \int_v [B]^T[\mathbf{C}^*_{ep}]\{\mathbf{A}_{12}\}\,\mathrm{d}v, \tag{28}$$

where $\{\mathbf{A}_{12}\}$ is a vector used in the derivation, and $[\mathbf{C}^*_{ep}]$ is the modified thermal elastic–plastic matrix.

The effect of LCF damage. When the load is applied cyclically during creep deformation process, the effect of LCF damage should be accounted for in the creep analysis [Yokobori and Sakata (1979) and Murakami and Sanomura (1986)]. In the implementation, this is achieved by calculating the LCF damage increment according to the plastic strain range within a load cycle [Degallaix *et al.* (1983)], and adding its amount to the current total accumulated damage.

Another important effect of the load cycling process on damage development is the redistribution of the stress field within the material. This stress redistribution has significant influence on subsequent creep evolution and damage development [Leckie and Hayhurst (1974) and Chen (1988)]. Also, when cracks are present in the material, stress redistribution reduces the degree of severity of the stress concentration around the crack tip region. Since the damage development and the creep evolution are all based on the current stress level, redistribution of the stress field would alter the development of damage and creep strain evolution, and eventually the failure of the overall structure.

The effect of load dwell time. During the load dwell time of the cyclic creep process, the material experiences certain microstructural changes. And also because of the permanent deformation which has already occurred within the material, when the load is exerted to the material again, the new creep strain rate in effect is no longer the same as the one before the load has been removed. This is referred to as the cyclic creep acceleration or cyclic creep retardation in literatures [Lorenzo and Laird (1984) and Gong and Hsu (1991)]. In the current implementation, this is reflected through the change of the maximum internal stress which represents the material's resistance to further creep deformation. Being a function of dwell time, the maximum internal stress affects the rates of the evolution of the internal stress and hence the damage parameter and the progress of creep deformation.

Interaction between creep and LCF. It has been found by many researchers that when the load is applied cyclically during the creep deformation process, the gradual material deterioration and the final failure of the material is caused not only by the creep damage and the LCF damage themselves, but also by the interaction between them [Yokobori and Sakata (1979) and Murakame and Sanomura (1986)]. In the present research, this is achieved through the summation of the damage caused in the creep deformation process and the damage caused in the LCF process within the same load cycle.

PARAMETRIC INVESTIGATION

The proposed CDM based model with the mixed EI algorithm is incorporated into the finite element program, TEPSAC, for thermal elastic–plastic stress analysis with creep. Before starting with the parametric study, the finite element implementation is checked against one-dimensional creep test results produced from specimens made out of 316L stainless steel [Gong and Hsu (1991)]. Figure 1 shows a good agreement with the static creep tests conducted at constant loadings of 165, 193, 221 and 231 MPa under a constant temperature of 650°C. Correlations with the creep strain results from a uniaxial bar subjected to a constant temperature of 650°C and cyclic mechanical load of 221 MPa is shown in Fig. 2, in which good agreement is observed. Having validated the model for simple configuration, the investigation of more complex two-dimensional creep problems is reported here.

For the three case studies conducted in this investigation, the material is 316L stainless steel, and the necessary input material constants are listed in Table 1. The loading conditions for the three case studies are shown in Fig. 3. The specimen is a thin panel with a center through crack. The geometry, dimensions of the panel and the mechanical loading pattern are illustrated in Fig. 4. The detailed finite element mesh around the crack tip region is shown in Fig. 5. Plane stress and constant strain elements are used in the analysis. A total of 199 elements and 166 nodes are used, and no special provisions are taken at the crack

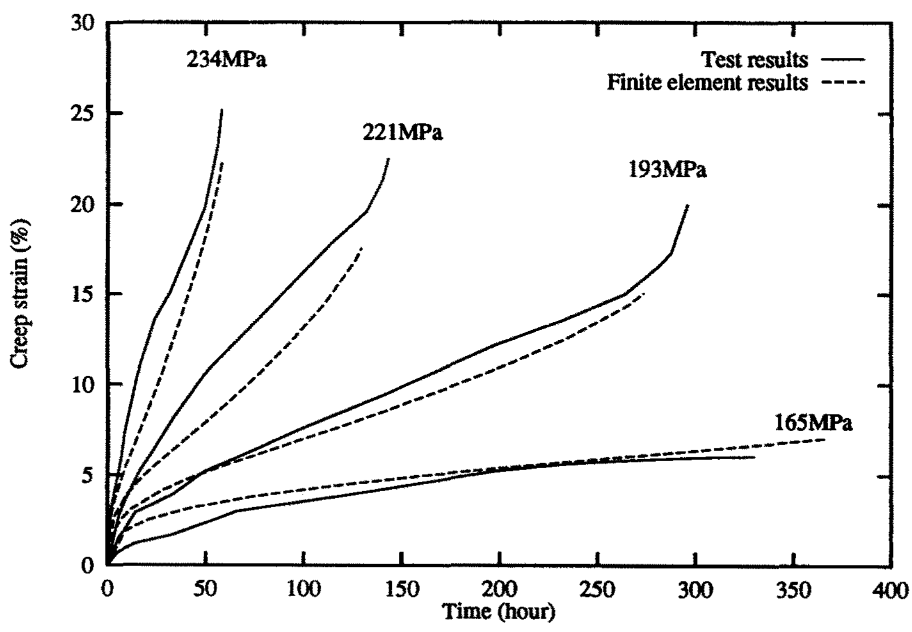

Fig. 1. Static creep strain development of 316L stainless bar at 650°C.

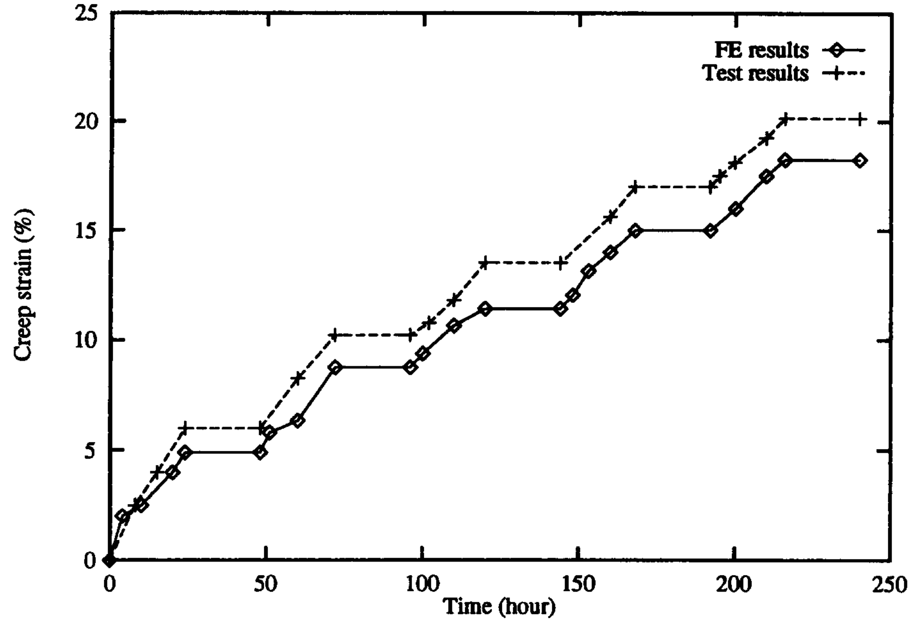

Fig. 2. Cyclic creep strain development of 316L stainless bar at 650°C, 221 MPa.

tip. To account for the relative high gradients of stress and strain in the crack tip region, very fine elements are deployed in the crack tip area and the expected crack extension path. In accordance with other CDM analysis, the crack extension criterion is assumed to be when the extrapolated damage parameter in the crack tip is equal to a critical value [Lemaitre (1985)]. In this analysis, the critical value is selected to be 0.98.

Case 1, *static creep analysis*

The case study was conducted to show the proposed model in describing static creep behavior. Without the interruption of the load cycling process and the load dwell time, it takes a longer incubation time for the crack to propagate.

Case 2, *cyclic creep without dwell time*

This case study was intended to check the importance of damage caused by the load cycling process during cyclic creep deformation. The load cycling process during creep deformation was found to be an important factor affecting the incubation time for the crack to grow and the subsequent crack growth rate, Not only did the load cycling process

Table 1. Input material parameters for 316L stainless steel

A	2.36×10^{-15}
$\mathbf{C}_1$	2.15×10^{-14}
$\mathbf{C}_2$	1.18×10^{-12}
n	5.84
r_o	0.711
$\mathbf{B}_1$	1.32×10^{2}
α	5.6×10^{-1}
β	1.80×10^{-2}
p	0.88
σ_n	1.00×10^{2}
$\mathbf{A}_1$	0.6445
$\mathbf{A}_2$	0.69×10^{-3}
$\mathbf{B}_3$	1.624
$\mathbf{B}_4$	1.792
Q	4.80 (K cal Mol^{-1})

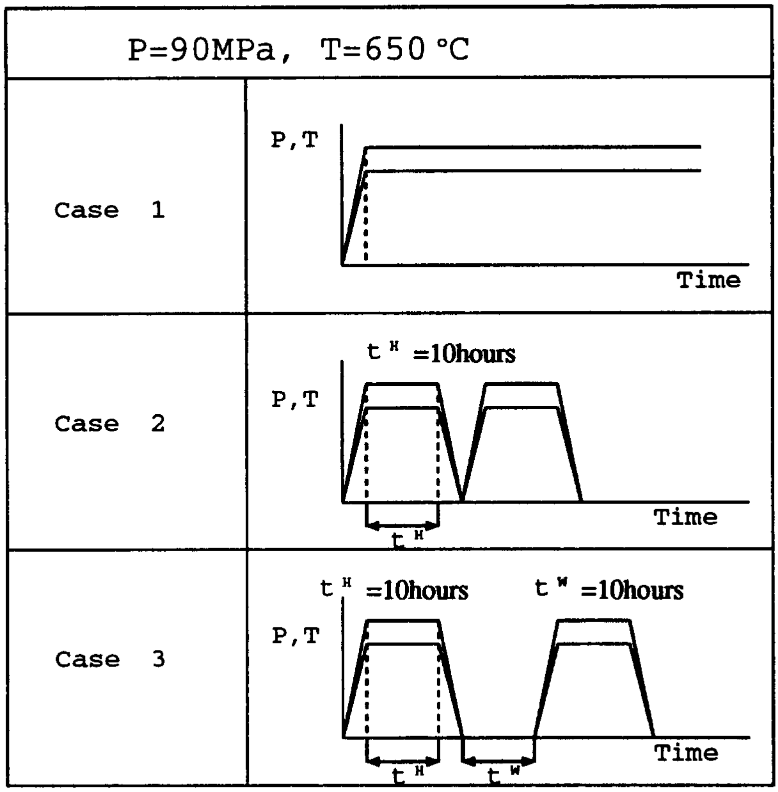

Fig. 3. Loading conditions for the case studies.

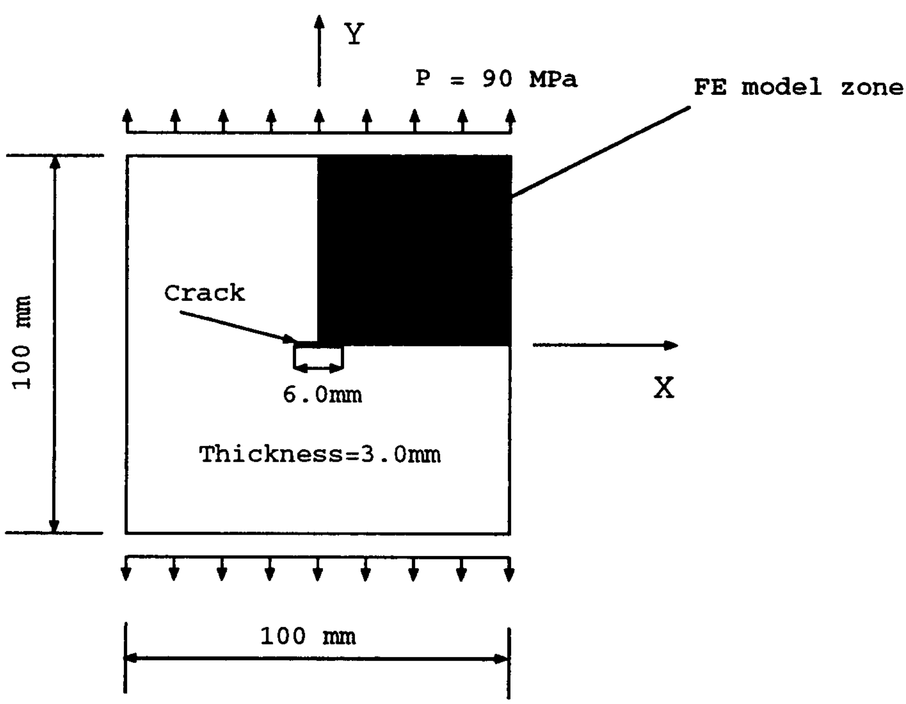

Fig. 4. Thin panel with center crack used for the case studies.

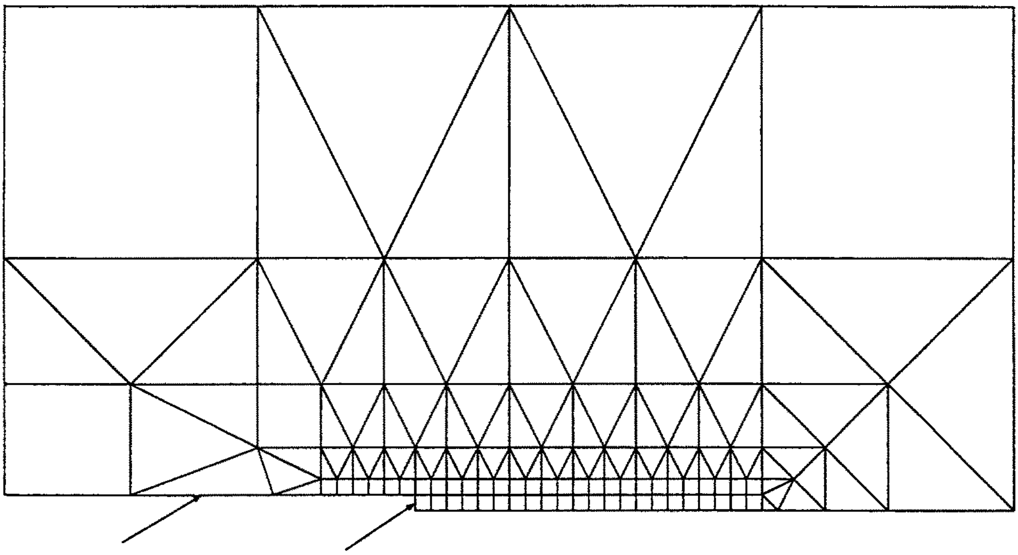

Fig. 5. Detailed FE mesh near crack tip for case studies.

introduce a certain amount of damage to the material directly but it also redistributed the stress field around the crack tip. This shows the same trend as in a previous analysis [Sun *et al.* (1992)]. This effect is essential for accurately assessing the deterioration of material because of the damage. Ignoring the damage caused by load cycling process in cyclic creep analysis will significantly over-estimate the life of the material.

Case 3, *cyclic creep with dwell time*

This case study was designed to monitor the load dwell time effect upon subsequent creep behavior in addition to the LCF damage effect for a complete cyclic creep analysis. The load holding time and the load dwell time were selected as 10 h.

OBSERVATIONS AND DISCUSSIONS

Case studies were performed using a new CDM based model with a mixed EI algorithm through finite element analysis. From the three loading conditions, i.e. static loading, cyclic loading without dwell time and cyclic loading with dwell time, it has been demonstrated that creep behavior is significantly affected by the profile and history of the applied loads. The load dwell time effect appears to be less important in comparison with the load cycling effect.

Both the load cycling process and the load dwell time have certain effects on subsequent creep evolution and damage development in the material. Furthermore, the incubation time for crack growth and the subsequent growth rate are also dependent on the type of loadings. The load dwell time effect is relatively small in comparison with the LCF influence on the overall response. However, because the selected duration of the load dwell time is relatively short (10 h) in this analysis, no conclusive observation could be made at this stage. Further studies are needed to compare the relative effect of LCF and load dwell time.

The evolution of the damage equivalent stress $\tilde{\sigma}$ in the near crack tip region was monitored and recorded for each case study because the damage equivalent stress is the controlling parameter for both creep strain evolution and damage development, its magnitude gives an overall picture of the activity at the crack tip. As the thermal and mechanical loads were applied to the panel, there was a significant stress concentration near the crack tip. When the creep deformation took place, the stress concentration became less severe due to the stress relaxation effect commonly encountered in viscoplasticity analysis. Also,

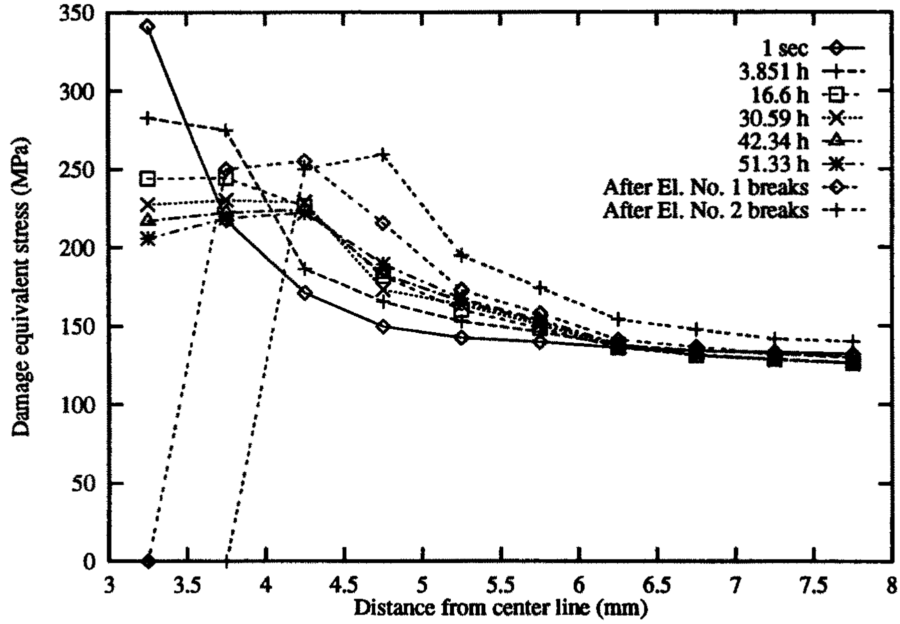

Fig. 6. Distribution of the damage equivalent stress near crack tip under static loading condition.

higher initial damage equivalent stress around the crack tip induces faster creep deformations. However, the deformation in the crack tip region is restrained by the surrounding area in which the creep strain is much lower. Consequently, unloading in the crack tip region occurs and the damage equivalent stress in the first few elements ahead of the crack tip drops.

Higher damage equivalent stress causes a larger damage rate. Consequently, damage in the first few elements ahead of the crack tip develops faster than in the surrounding elements. As the damage develops, the material becomes softer and less creep resistant. When the damage accumulates to a certain level, the material becomes too soft to withstand

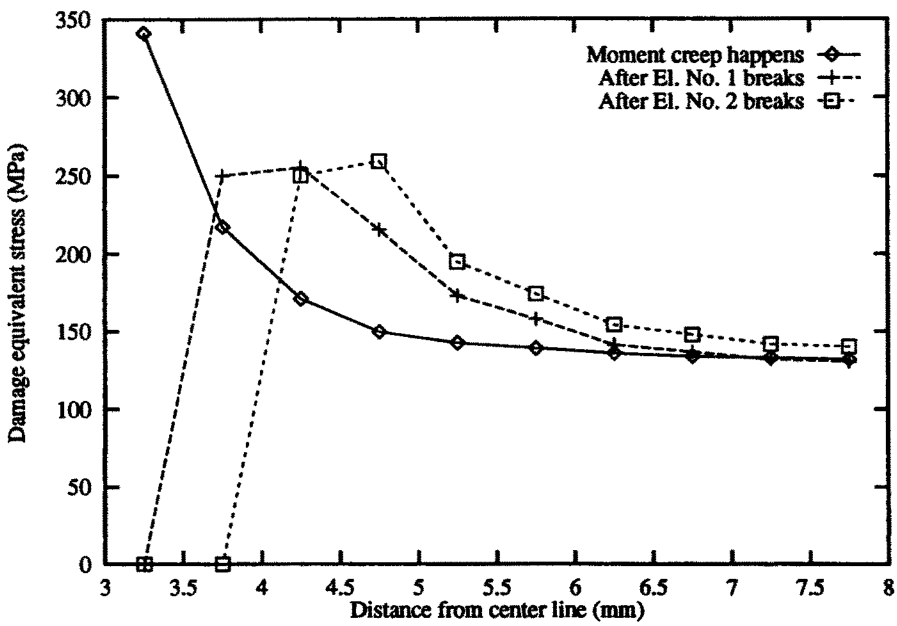

Fig. 7. Distribution of the damage equivalent stress ahead of a moving crack tip.

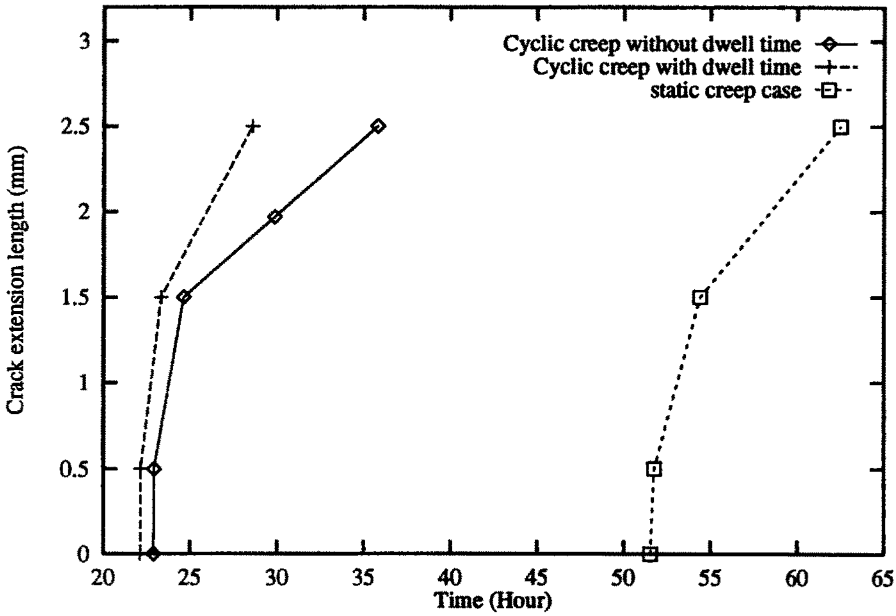

Fig. 8. Crack extension histories for the three case studies.

high damage equivalent stress. Mathematically, this means the accumulated damage approaches a numerical value of unity. Figure 6 shows the evolution of the damage equivalent stress ahead of the crack tip for the static creep case. The evolution of the damage equivalent stress ahead of a moving crack tip, as further illustrated in Fig. 7, shows a similar trend to the Chaboche's analysis results (1988). Figure 8 shows the crack extension histories for the three different loading conditions. The cyclic loading with both load holding time and load dwell time appeared to be most damaging. Under such loading conditions, the incubation time for the crack to propagate is shorter and the rate of crack growth is higher. However, the results under cyclic loading with and without dwell time did not make much

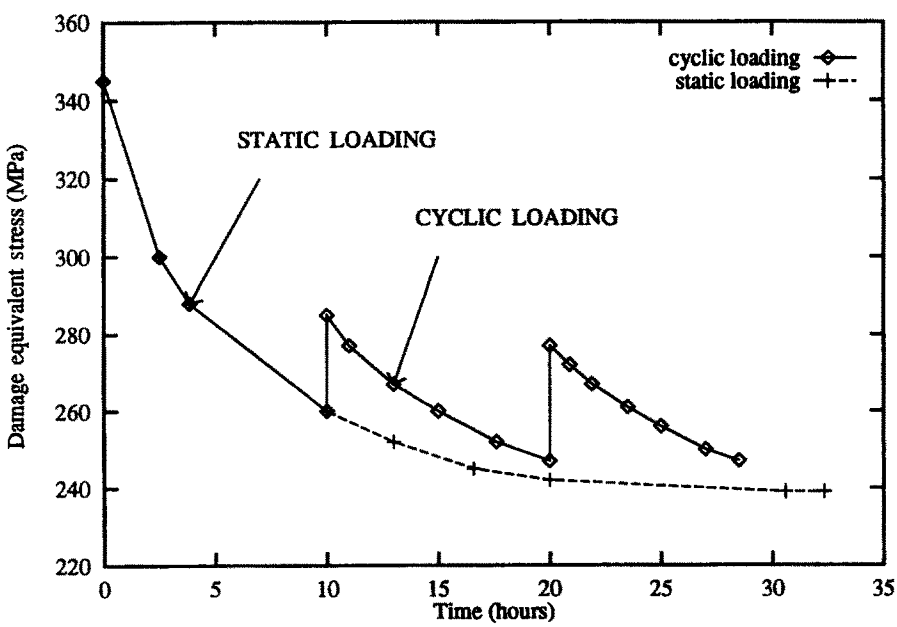

Fig. 9. Development of the damage equivalent stress under static and cyclic loading conditions.

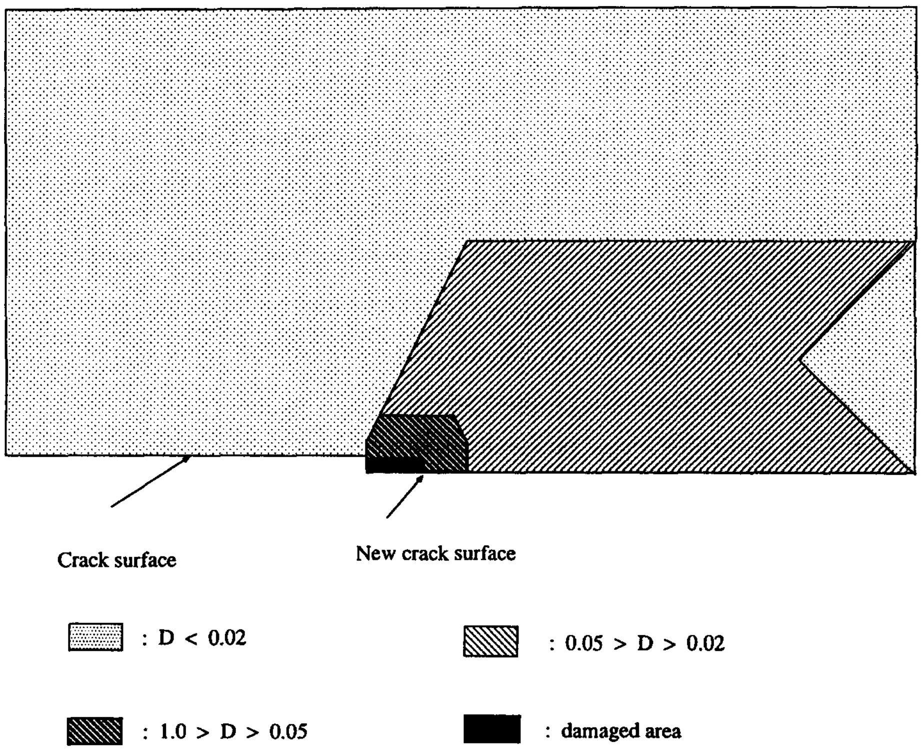

Fig. 10. Damage zone near a crack tip.

difference. Figure 9 shows the evolution of the damage equivalent stress in time in the crack tip area under both cyclic and static loading conditions. The load cycling process redistributes the stress field in the crack tip area. The damage equivalent stress under cyclic loading is always higher than that of static loading. This is essentially the reason why cyclic loading is more damaging than the static loading. Figure 10 shows the damage pattern around the crack tip area after the crack tip has made certain advances. The material near the crack tip experienced severe damage. This area also hosts higher stress. The damage pattern reported here is quite similar to the results of other researchers [Lemaitre (1985) and Chaboche (1988)].

Systematic correlations with experimental test results, for both one-dimensional and two-dimensional specimens subjected to various cyclic loading patterns, will be presented in another paper.

Acknowledgements—The authors acknowledge the financial support of the Natural Sciences and Engineering Research Council of Canada. Numerous discussions and many useful suggestions made by Drs G. G. Chen (Manitoba Research Council) and Z. L. Gong (Monac International Co.) are gratefully acknowledged.

REFERENCES

Boyle, J. T. and Spence, J. (1983). *Stress Analysis for Creep*. Butterworth–Heinimann, Oxford.

Chaboche, J. L. (1988). Continuum damage mechanics, part 1 and part 2. *J. Appl. Mech.* **55**, 59–72.

Chen, G. G. (1988). Creep crack growth under cyclic loading conditions, a continuum damage approach, Ph.D Thesis, University of Manitoba.

Chen, G. G. and Hsu, T. R. (1988). A mixed explicit-implicit (EI) algorithm for creep stress analysis. *Int. J. Numer. Meth. Engng* **26**, 511–524.

Chow, C. L. and Wang, J. (1987). An anisotropic theory of continuum damage mechanics for ductile fracture. *Engng Fract. Mech.* **27**, 547–558.

Cormeau, I. (1975). Numerical stability in quasi-static elasto/visco-plasticity. *Int. J. Numer. Meth. Engng* **9**, 109–127.

Degallaix, G. *et al.* (1983). A damage law for predicting the elevated temperature low cycle fatigue life of a Martensitic stainless steel. *Mater. Sci. Engng* **58**, 55–62.

Degallaix, G. *et al.* (1990). Lifetime prediction on Cr-Mo-V and 316L steels under thermal and mechanical cycling, fatigue frac. *Engng Mater. Struct.* **13**, 473–485.

Gong, Z. L. and Hsu, T. R. (1991). A constitutive model for metals subjected to cyclic creep. *J. Engng Mater. Tech., ASME Trans.* **113,** 419–424.

Hsu, T. R. (1986). *The Finite Element Method in Thermomechanics.* Allen and Unwin, Boston.

Hughes, T. J. R. and Liu, W. K. (1978). Implicit-explicit finite elements in transient analysis: stability theory. *J. Appl. Mech.* **45,** 371–374.

Hughes, T. J. R. and Taylor, R. L. (1978). Unconditionally stable algorithms for quasi-static elasto/visco-plastic finite element analysis. *Comp. Struct.* **8,** 169–173.

Kachanov, L. M. (1958). On the creep fracture time. *Izu, AN SSR, Otd. Tekhn. Nauk* **8,** 26–31 (in Russian).

Krajcinovic, D. and Fonseka, G. U. (1981). The continuous damage theory of brittle materials, part 1 and part 2. *J. Appl. Mech.* **48,** 809–824.

Landes, J. D. and Begley, J. A. (1976). A fracture mechanics approach to creep crack growth, mechanics of crack growth, *ASTM STP* **590,** 128–148.

Leckie, F. A. (1980). Advance in creep mechanics. In *Proc. IUTAM Symp.* pp. 13–65 Leicester, U.K.

Leckie, F. A. and Hayhurst, D. R. (1974). Creep rupture of structures. *Proc. R. Soc. London* **A. 340,** 323–347.

Leeuwen, H. P. V. (1977). The application of fracture mechanics to creep crack growth. *Engng Fract. Mech.* **9,** 951–974.

Lemaitre, J. (1985). A continuous damage mechanics model for ductile fracture. *J. Engng Mater. Tech.* **107,** 83–89.

Levy, A. and Pifko, A. B. (1981). On computational strategies for problems involving plasticity and creep. *Int. J. Numer. Meth. Engng.* **17,** 747–771.

Liu, W. K. and Lin, J. I. (1982). Stability of mixed time integration schemes for transient thermal analysis. *Numer. Heat Transfer* **5,** 211–222.

Lorenzo, F. and Laird, C. (1984). Cyclic creep acceleration and retardation in polycrystalline copper tested at ambient temperature. *Acta. Metall.* **132,** 681–692.

McEvily, A. J. and Wells, C. H. (1973). On the applicability of fracture mechanics to elevated temperature design. *Inst. Mech. Engrs* **C230/73,** 230.1–230.7

Miller, A. (1976). An inelastic constitutive model for monotonic, cyclic and creep deformation, part 1 and part 2. *J. Engng Mater. Tech.* **98,** 97–113.

Mroz, Z. (1967). On the description of anisotropic workhardening. *J. Mech. Phys. Solids* **15,** 163–175.

Murakami, S. (1983). Notion of continuum damage mechanics and its application to anisotropic creep damage theory. *J. Engng Mater. Tech.* **105,** 99–105.

Murakami, S. and Sanomura, Y. (1986). Analysis of the coupled effect of plastic damage and creep damage in Nimonic 80A at finite deformation, *Engng Fract. Mech.* **25,** 693–704.

Nicholson, R. D. and Formby, C. L. (1975). The validity of various fracture mechanics methods at creep temperatures. *Int. J. Fract.* **11,** 595–604.

Nikbin, K. M., Webster, G. A. and Turner, C. E. (1976). Relevance of nonlinear fracture mechanics to creep cracking. In *Cracks and Fracture, ASTM STP 601,* pp. 47–62.

Odqvist, F. K. G. (1980). Historical survey of the development of creep mechanics from its beginnings in the last century to 1970. In *Proc. IU TAM Symp.* pp. 1–12, Leicester, U.K.

Plumtree, A. (1977). Creep/fatigue interaction in type 304 stainless steel at elevated temperature, *Metal Sci.* **11,** 425–431.

Rabotnov, Yu. N. (1969). *Creep Problems in Structural Members.* North-Holland, New York.

Saxena, A. (1980). Evaluation of C^* for the characterization of creep-crack-growth behavior in 304 stainless steel. In *Fracture Mechanics: Twelfth Conf. ASTM STP 700,* pp. 131–151.

Smith, S. D., Webster, J. J. and Hyde, T. H. (1989). Finite element investigation of creep crack growth from surface thumbnail cracks. *Engng Fract. Mech.* **34,** 625–635.

Sun, B. K. *et al.* (1992). A continuum damage mechanics model for cyclic creep fracture. Internal report, Department of Mechanical Engineering, University of Manitoba.

Tanaka, T. G. and Miller, A. K. (1988). Development of a method for integrating time-dependent constitutive equations with large, small or negative strain rate sensitivity. *Int. J. Numer. Meth. Engng* **26,** 2457–2485.

Yokobori, T. and Sakata, H. (1979). Studies on crack growth rate under high temperature creep, fatigue and creep-fatigue interaction, part 1 and part 2. *Engng Fract. Mech.* **13,** 509–532.

Yokobori, A. T. and Yokobori, T. (1988). The crack initiation and growth under high temperature creep, fatigue and creep-fatigue multiplication. *Engng Fract. Mech.* **31,** 931–945.